Romanian Reports in Physics, Vol. 63, No. 3, P. 729–740, 2011

RESIDUAL RADIOACTIVITY INDUCED BY PROTONS AND ^{12}C IONS IN BIOMEDICAL MATERIALS

A. MIHAILESCU[1,2], N. VERGA[3], M.A. POPOVICI[2], L. STRASSER[2], D. FILIPESCU[4] GH. CĂTA-DANIL[2,4]

[1]Department of Physics, Faculty of Chemistry, University of Bucharest, 4-12 Bd. Elisabeta, 030018 Bucharest, Romania
E-mail: alex2hr@yahoo.com
[2]Department of Physics, University "Politehnica"of Bucharest, 313 Splaiul Independentei, 060042 Bucharest, Romania
[3]Department of Oncology, "Carol Davila" University of Medicine, Bd. Dionisie Lupu 37, 020021 Bucharest, Romania
[4]"Horia Hulubei" National Institute for Physics and Nuclear Engineering, P.O. Box MG-6, Bucharest, Romania

Received January 10, 2011

Abstract. Residual radioactivity following the charged particle irradiations of biomedical materials was measured with a high resolution HPGe spectrometer. Proton and ^{12}C ion beams delivered by the Bucharest FN Tandem Van de Graaff accelerator bombarded bone and artificial heart valve samples at the beam energies comparable with those reached in hadron therapy near the Bragg peak region. Energies, relative intensities and decay curves of the delayed gamma rays following irradiation are reported in the present work. Statistical model calculations for all possible nuclear reactions likely to occur in these experiments were performed by using Talys 1.0 and Cascade codes. These results provide new spectrometric data relevant for the study of the potential late radiation effects from particle radiation exposures in medical therapy.

Key words: residual radioactivity, proton and heavy ion induced reactions, gamma ray production, biomedical materials.

1. INTRODUCTION

Novel techniques applied for the local tumor therapy have been developed in the last decades by using for irradiations charged hadron beams (protons, heavy ions) instead of the conventional X rays and electrons. The advantages of these procedures are tied up with accurate localization of the deposited energy in tissues (Bragg peak) and a larger biological efficiency [1, 2, 3].

Unlike proton beams, heavier ions supply a grater biological efficiency because of their Linear Energy Transfer (LET) and consequently increased relative biological efficiency (RBE) at the end of their range. In order to treat deep seated

tumors, beams with incident energies in the 100 MeV/u range are required. Just before the particles stop an increase of the linear energy deposition occurs – the Bragg peak, whose position within tissues is fully controllable by the incident beam energy [4, 5].

In the Bragg peak region the beam energy decreases to MeV/u range leading to nuclear reactions which involve direct, compound nucleus and preequilibrium mechanisms [6].

In the present paper experimental and theoretical results on the residual radioactivity occurring after the irradiation with a 8 MeV proton beam of a bone sample and 44.4 MeV ^{12}C ion beam of an artificial heart valve sample are presented. Proton and ^{12}C ion beams were delivered by the Tandem Van de Graaff accelerator at the IFIN-HH, Bucharest and delayed gamma rays were measured with high resolution HPGe gamma-ray spectrometers. Model calculations of the cross sections for the produced residual nuclei are performed with the computer codes Talys 1.0 [7] and Cascade [8]. Gamma ray energies and their relative intensities together with the decay curves for the strongest lines emitted by the radioactive nuclei are reported. These results provide new spectrometric information relevant for the dosimetric evaluations in the Bragg peak region [9,10].

2. BONE SAMPLE IRRADIATED WITH PROTONS

A 1 mm thick bone probe prepared at the oncologic centre of Coltea Hospital was irradiated with 8 MeV proton beams delivered by the Tandem Van de Graaff accelerator for about 100 minutes. The current beam on the target was ~8 nA. SRIM calculations [11] estimate a value of the projected range smaller than 1 mm so the beam completely stops in the target volume. After 15 minutes of cooling time gamma spectra of the irradiated sample were recorded for 2 hours in 100 sec intervals with a 30% efficiency HPGe detector. A second measurement of the gamma spectra for the same sample was performed about 60 hours later at the LaMAR laboratory (UPB) with a 30% efficiency HPGe detector mounted in a lead shield, in order to detect gamma emissions with longer half-lives. Background and calibration standard sources (^{152}Eu, ^{60}Co) were also measured.

2.1. SHORT COOLING TIME SPECTRA ANALYSIS

Measured single spectra are summing-up contributions from gamma rays originating from the irradiated sample and those from the laboratory background. In Fig. 1 recorded gamma spectrum at the end of the 2 hours acquisition time is presented. Peak deconvolution from the recorded spectra was performed with LEONE package [12] and efficiency corrections were performed with the ^{152}Eu

gamma source. The energy resolution vary from 1.2 keV FWHM at 122 keV up to 2.2 keV FWHM at 1408 keV. The background gamma lines is due mainly to the natural radioactivity of the ^{238}U(^{226}Ra) and ^{232}Th series.

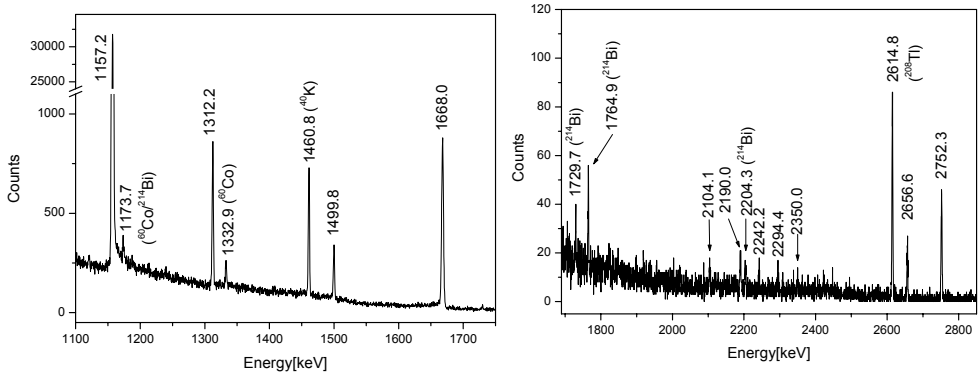

Fig. 1 – Examples of gamma spectra measured for the bone sample 15 min after the irradiation stopped at the Tandem laboratory. The background gamma lines are labeled by the emitting nuclei. The parent nucleus is assigned to each known gamma line.

After eliminating the background, gamma ray relative intensities were calculated by correcting the peak areas with the efficiency values. In Table 1 are presented the relative intensities normalized to the value of the 1157.2 keV gamma-ray transition ($I_{1157.2}$≡100).

Table 1

Observed gamma rays induced by the decaying of the nuclei formed by proton irradiation on the bone sample, arranged in order of increasing energy (E_γ). Their intensities (I_{rel}) are normalized to the one of the 1157.2 keV transition (**$I_{1157.2}$≡100)**

E_γ(keV)	**I_{rel}**	**E_γ(keV)**	**I_{rel}**
372.8	1.11(8)	2190.0	0.07(1)
983.7	2.43(6)	2242.2	0.02(1)
1037.8	2.42(5)	2294.4	0.02(1)
1157.2	**100.00(23)**	2350.0	0.03(1)
1312.3	2.42(4)	2656.6	0.09(1)
1499.8	0.87(3)	2752.3	0.24(1)
1668.0	4.76(6)		

2.2. LONG COOLING TIME SPECTRA ANALYSIS

In Fig. 2 are presented gamma spectra of the bone sample measured about 60 hours after irradiation stop.

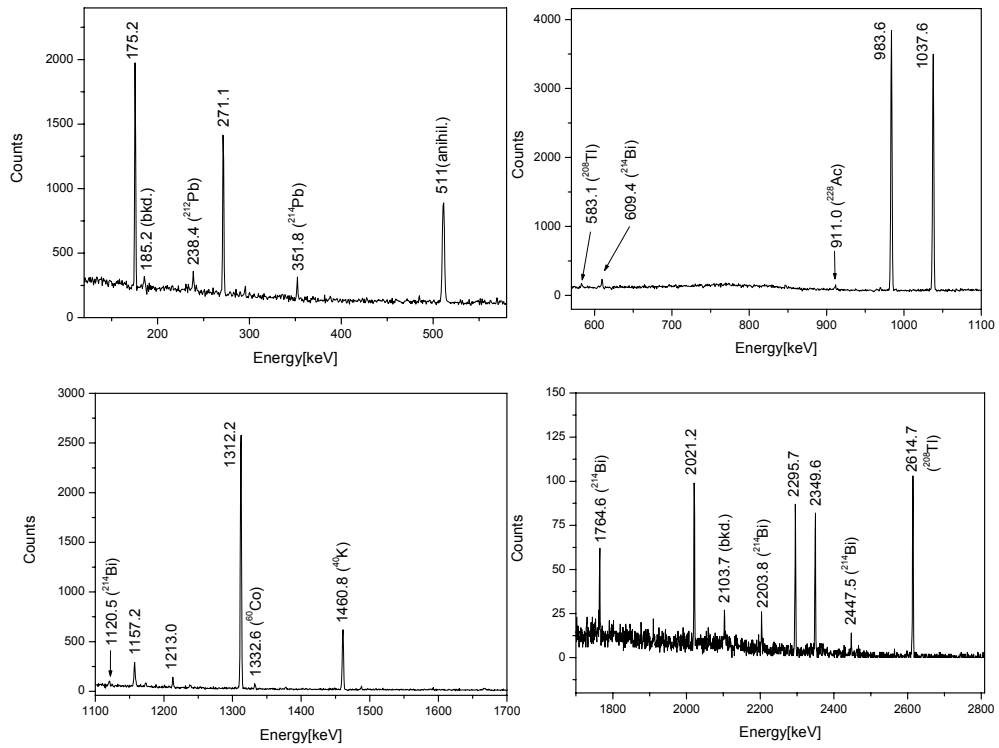

Fig. 2 – Gamma ray spectra of the bone sample 60 hours after irradiation measured in the LaMAR laboratory. Most of the background gamma lines are emitted due to the natural radioactivity of the ^{238}U(^{226}Ra) and ^{232}Th series.

By selecting only the gamma lines of the bone probe one notice that there are few gamma lines left namely 175.2, 271.1, 983.6, 1037.6, 1157.2, 1213.0, 1312.2, 2021.2, 2295.7 and 2349.6 keV that are emitted by nuclides with half-lives of order of days or longer.

2.3. RADIOACTIVE NUCLEI IDENTIFICATION

In order to identify the decaying nuclei two kind of arguments were used. The first one was based on the results of statistical model calculations of cross sections performed by computer code Talys 1.0 and the second one used the

experimentally determined decay curves of the gamma lines. For nuclear model parameters were employed default code values [13, 14]. Statistical model calculations for proton reactions on Ca nuclides shown that the most likely reactions leading to gamma emitting nuclei are p+^{43,44,46,48}Ca. The strongest open reaction channels predicted were as follows: (*p,p*) for p+^{40,42}Ca and (*p,n*) for p+^{43,44,46,48}Ca. According to the ENSDF-NNDC [15] nuclear data, only few reactions leading to ^{43,44}Ca, ^{44}Sc and $^{46\text{-}49}$Ti nuclides are followed by delayed gamma emission. In Table 2 are presented comparatively the experimental gamma energy values with ENSDF data together with the emitting nuclides.

Table 2

Comparison of the gamma ray energies between experimental (present work) and ENSDF data file and assignation of the emitting nucleus. PN[$T_{1/2}$] is the parent nucleus together with the half life value from ENSDF (DN is the daughter nucleus; uncertainties are of the order of last digit)

E_{exp}(keV)	E_{ENSDF}(keV)	PN[$T_{1/2}$]	DN
372.8	372.76	^{43}Sc[3.891(12)h]	^{43}Ca
271.1	270.9	^{44m}Sc[58.61(10)h]	^{44}Sc
1157.2	1157.02	^{44}Sc[3.97(4)h]	^{44}Ca
1499.8	1499.46	^{44}Sc[3.97(4)h]	^{44}Ca
2656.6	2656.48	^{44}Sc[3.97(4)h]	^{44}Ca
175.2	175.36	^{48}Sc[43.67(9)h]	^{48}Ti
983.7	983.53	^{48}Sc[43.67(9)h]	^{48}Ti
1037.8	1037.52	^{48}Sc[43.67(9)h]	^{48}Ti
1213.0	1212.88	^{48}Sc[43.67(9)h]	^{48}Ti
1312.3	1312.12	^{48}Sc[43.67(9)h]	^{48}Ti

The EC decay ^{41}Ca-^{41}K occurring from the p+^{40,41}Ca reactions is not followed by gamma emission [15]. The β^- decay ^{45}K-^{45}Ca occurring from the p+^{48}Ca reaction is followed by gamma emission but not observed in the present experiment due to the cooling time which is approximately the same with the half life of the parent nuclide and the channel (*p,α*) is four orders of magnitude smaller than the (*p,n*) channel. The β^- decay ^{45}Ca-^{45}Sc is accompanied by a single gamma line of 12.47 keV not observable. The β^- decay ^{46}Sc-^{46}Ti occurring from the p+^{46}Ca reaction is followed by 3 gamma lines not observable probably due to the small abundance of the ^{46}Ca isotope. The β^- decay ^{47}Sc-^{47}Ti occurring from the p+^{46}Ca reaction is accompanied by a single gamma line 159.381 keV not observable in the spectrum due to the small abundance of the ^{46}Ca isotope; in addition the ^{47}Sc nucleus is formed by proton capture channel which is very small comparing to the (*p,n*)

channel. The β^- decay ^{49}Sc-^{49}Ti occurring from the p+^{48}Ca reaction, two gamma lines namely 1662.6 and 1761.9 keV are emitted but not observed in the present experiment probably due to their very low intensities [15]. Another reason is that the ^{49}Sc nucleus is formed by proton capture channel which is of 3 orders of magnitude smaller comparing to the (*p,n*) channel.

2.4. HALF LIFE MEASUREMENTS

The half life was extracted from the experimental decay curves of the gamma lines. The half life for the ^{44}Sc nucleus was calculated using its 1157.2 keV most intense gamma line. The ground state 2^+ is reached by the emission of the 270.9 keV gamma line from the isomeric transition (98.80%) and then the nucleus decays by electron capture reaching the ground state of the stable ^{44}Ca nucleus. In order to calculate the half life, gamma spectra were recorded in 100 sec intervals. The radiation emitted during each 100 sec interval was calculated by means of peak area subtractions. Assuming in a rough approximation that the activity is constant over 500 s (~8 min), the value of the half time was found to be 7.21(482)h (Fig. 3b) which fairly agrees with the adopted one of 3.97(4)h [15].

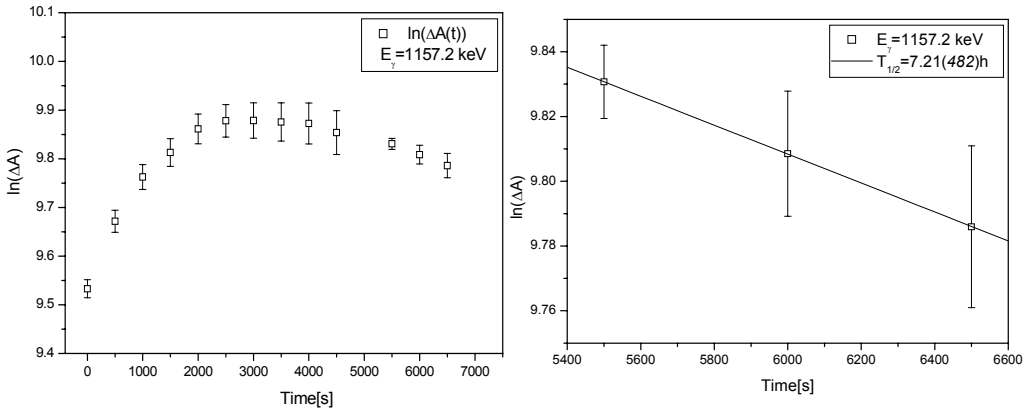

Fig. 3 – a) The decay curve of the 1157.2 keV gamma ray from the ^{44}Sc nucleus; b) the half time value was calculated from the slope of the decay curve plotted by interpolating the experimental points that shown a linear regression. ΔA represents the subtracted peak area.

The uncertainty of the measurements was determined mainly by the acquisition time.

3. ARTIFICIAL HEART VALVE SAMPLE IRRADIATED WITH ^{12}C IONS

The 1 mm thick artificial heart valve sample made of pyrolytic carbon was irradiated with 44.4 MeV ^{12}C ion beam. According to SRIM calculations the

projected range is 0.05 mm therefore the beam stops completely in the target volume. After 20 minutes of cooling time gamma spectra of the irradiated sample started to be recorded for 8 hours in 100 s intervals with a 30% efficiency HPGe detector.

3.1. SHORT COOLING TIME SPECTRA ANALYSIS

In Fig. 4a gamma spectrum taken with the longest acquisition time is presented.

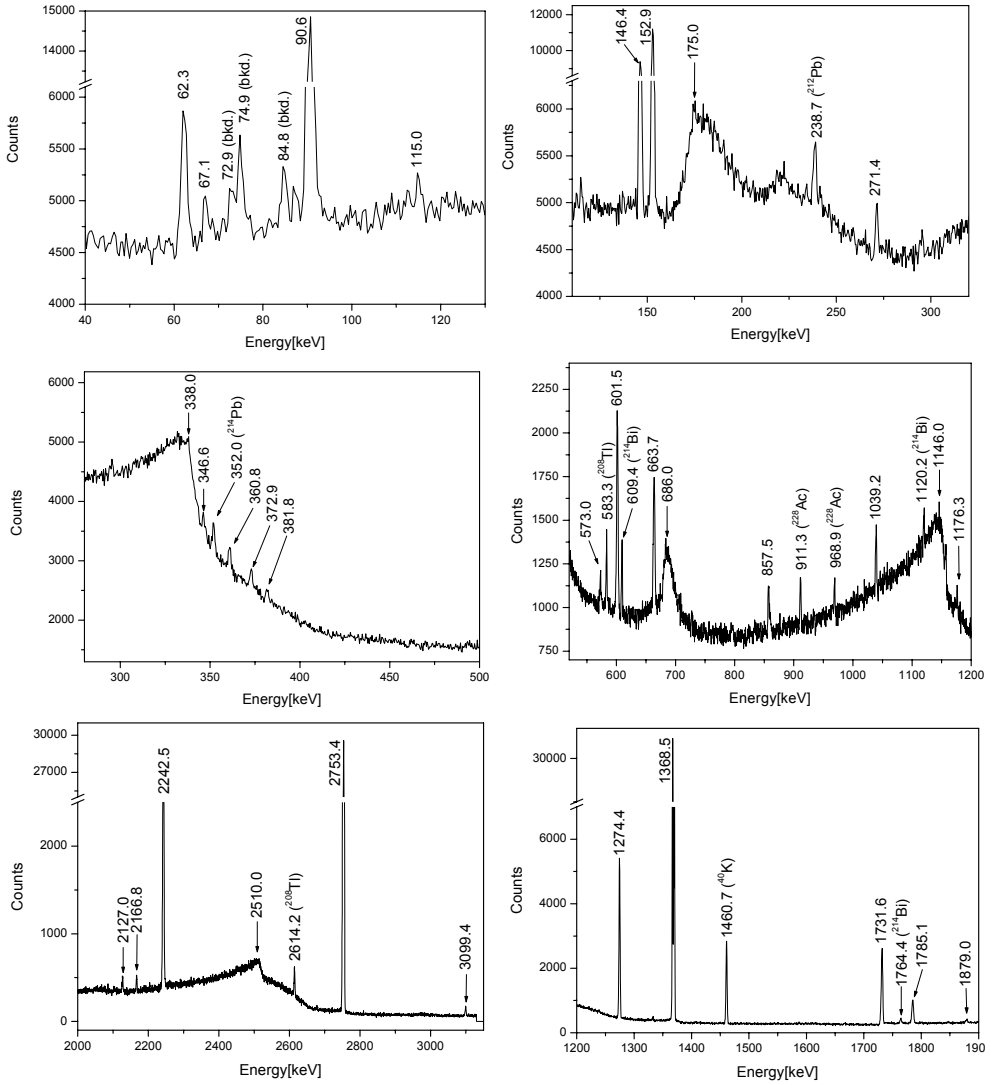

Fig. 4 – Gamma spectra emitted by the artificial heart valve sample 20 min after the irradiation stopped. The background gamma lines are labeled by the emitting nuclei. See text for details.

After eliminating of the background the gamma ray relative intensities were calculated by correcting the peak areas with the efficiency values. In Table 3 are presented the relative intensities normalized to the one of the 1368.5 keV ($I_{1368.5}$≡100).

Table 3

Observed gamma rays induced by the decaying of the nuclei formed by ^{12}C irradiation on the artificial heart valve target, arranged in order of increasing energy (E_γ). Intensities are normalized to the one of the 1368.5 keV transition (**$I_{1368.5}$≡100)**

E_γ(keV)	**I_{rel}**	**E_γ(keV)**	**I_{rel}**
62.3	0.24(1)	857.5	0.24(2)
67.1	0.06(1)	1039.2	0.33(2)
90.6	1.94(1)	1176.3	0.07(1)
115.0	0.06(1)	1274.4	5.89(4)
146.4	0.93(1)	**1368.5**	**100.00(15)**
152.9	1.39(1)	1731.6	4.20(3)
271.4	0.10(1)	1785.1	1.57(3)
346.4	0.08(1)	1879.0	0.23(2)
360.8	0.11(2)	2127.0	0.29(2)
372.9	0.08(1)	2166.8	0.28(2)
381.8	0.04(1)	2242.5	9.05(5)
573.0	0.08(1)	2753.4	59.71(12)
601.5	0.93(2)	3099.4	0.21(1)
663.7	0.75(2)		

3.2. LONG COOLING TIME SPECTRA ANALYSIS

A second measurement of the gamma spectra was performed about 60 hours after irradiation at the LaMAR laboratory (UPB) with a 30% efficiency HPGe detector. In Fig. 5 is presented the gamma ray spectra recorded from the artificial heart valve 60 hours after irradiation.

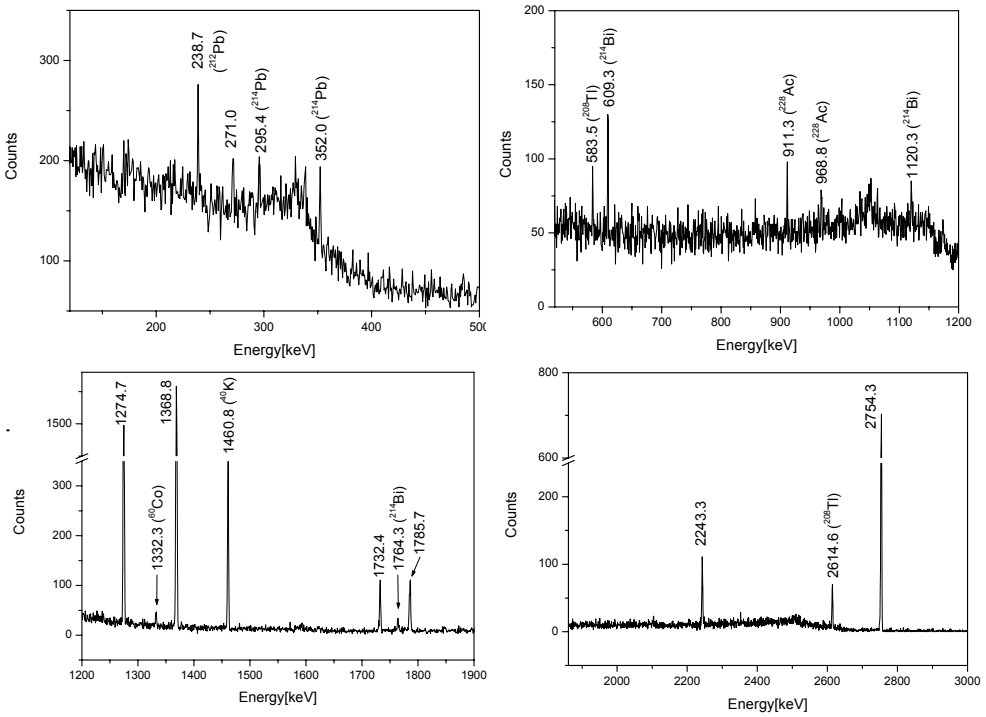

Fig. 5 – Gamma ray spectra of the artificial heart valve sample 60 hours after irradiation measured in the LaMAR laboratory. The background gamma lines are labeled by the emitting nuclei.

After eliminating the background gamma lines one can notice that there are few gamma lines namely 2 71.0, 1 274.7, 1 368.8, 1 732.4, 1 785.7, 2 243.3 and 2 754.3 keV that are emitted by nuclides with half-lives of order of days or longer.

3.3. RADIOACTIVE NUCLEI IDENTIFICATION

Model calculations were performed with the computer code CASCADE for the ^{12}C+^{12}C reaction according to the sample main composition. The code predicts all channels to be open based on the Hauser-Feshbach compound nucleus formalism [16]. Default nuclear model parameters were employed.

Table 4

Cross sections calculations (mb) estimated with the computer code CASCADE for the ^{12}C+^{12}C reaction. PN /DN is the parent/daughter nucleus. $T_{1/2}$ values are from ENSDF [15]

Open channel	**Present work**	**PN**	**$T_{1/2}$**	**DN**
n2α	1.353	^{15}O	122.24(16)s	^{15}N
p2α	9.489	^{15}N		

Table 4 (continued)

2α	333	^{16}O		
αn	34.08	^{19}Ne	17.22(2) s	^{19}F
αp	126.4	^{19}F		
α	111.1	^{20}Ne		
n2p	15.92	^{21}Ne		
2n	1.522	^{22}Mg	3.8755(12)s	^{22}Na
pn	192	^{22}Na	2.6027(10) y	^{22}Ne
2p	94.87	^{22}Ne		
n	8.552	^{23}Mg	11.317(11)s	^{23}Na
p	20.36	^{23}Na		

According to Cascade calculations for ^{12}C beam bombarding the ^{12}C target nucleus only the 1 274.4 keV gamma line from the ^{22}Na-^{22}Ne decay is expected to be observed. However other nuclei are expected to be found in the target.

In Fig. 6 are presented experimental data for calculating half-lives in order to identify of the occurring nuclei during irradiation.

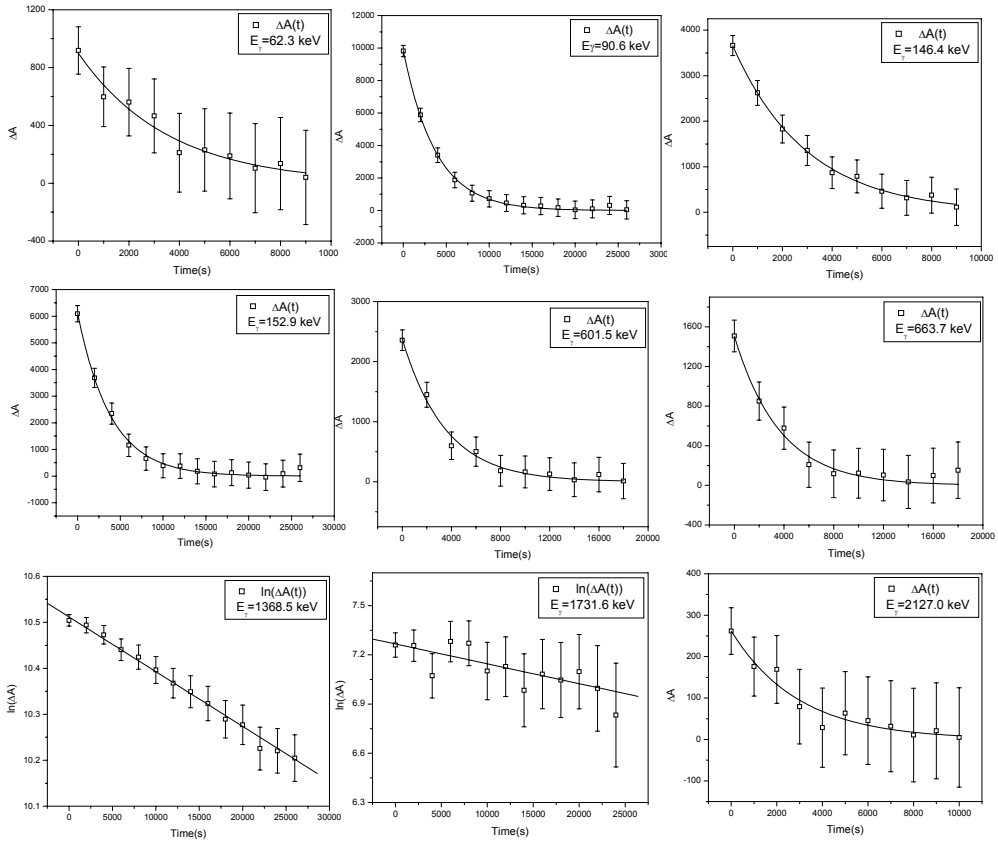

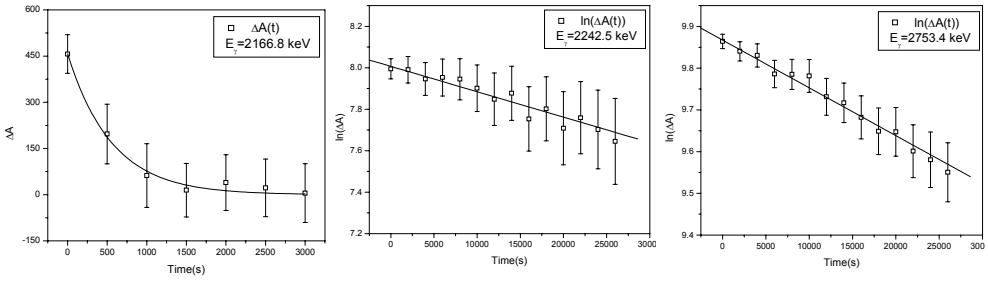

Fig. 6 – The experimental radioactivity over the 8 hours spectra acquisition by means of the gamma lines emitted. Half-lives were extracted either by interpolating the experimental points by a first degree decaying exponential curve for short lifetimes or by means of the slope method derived from a linear regression for long lifetimes. ΔA and E_γ represent the subtracted peak area and the peak energy respectively.

The experimental results for the half lives are presented in Table 5.

Table 5

Calculated half-lives for different nuclides formed after irradiation with ^{12}C ions. A comparison between experimental gamma energy and half life values from the present work and ENSDF values is presented. $T_{1/2exp}$ is the present work half life value extracted from the interpolated data points and PN[$T_{1/2}$] is the parent nucleus together with the half life values taken from the ENSDF data file. DN is the daughter nucleus

E_{exp}(keV)	E_{ENSDF}(keV)	$T_{1/2exp}$	PN[$T_{1/2}$]	DN
62.3	62.298	41.6(37)m	^{49}Cr[42.3(1)m]	^{49}V
90.6	90.639	40.2(43)m	^{49}Cr[42.3(1)m]	^{49}V
146.4	146.36	34.3(43)m	^{34m}Cl[32.00(4)m]	^{34}Cl
152.9	152.928	44.9(48)m	^{49}Cr[42.3(1)m]	^{49}V
1368.5	1368.626	15.7(3)h	^{24}Na[14.997(12)h]	^{24}Mg
2127.0	2127.492	33.9(38)m	^{34}Cl[32.00(4)m]	^{34}S
2166.8	2167.5	7.0(5)m	^{38}K[7.636(18)m]	^{38}Ar
2753.4	2754.007	15.8(6)h	^{24}Na[14.997(12)h]	^{24}Mg

The 2 242.5 ($T_{1/2exp}$=14.7(13)h) and 1 731.6 keV ($T_{1/2exp}$=14.1(32)h) lines are the single and double escape respectively of the 2753.4 keV peak associated with ^{24}Na. The 1 176.3 keV line (half-life not calculated) is assigned to the ^{34}Cl-^{34}S EC decay. The 857.5 and 346.4 keV lines are the single and double escape respectively of the 1 368.5 keV peak associated with ^{24}Na. The 1 785.1 keV line is a sum peak relative to the 1 274.4 keV line emitted in the ^{22}Na-^{22}Ne β^+ decay. The 573.0, 601.5

($T_{1/2exp}$=40.3(25)m) and 663.7 ($T_{1/2exp}$=42.3(45)m) keV lines are the sum peaks relative to 62.3, 90.6 and 152.9 keV lines respectively emitted in the ^{49}Cr-^{49}V β^+ decay.

4. CONCLUSIONS

Residual radioactivity based on the delayed gamma rays arising from the exposure of a bone sample to an 8 MeV proton beam and of a artificial heart valve sample to a 44.4 MeV ^{12}C ion beam have been measured by using high resolution gamma ray spectroscopy. Gamma ray energies, relative intensities together with some values of half lives of the identified residual nuclei are reported. Predictions for the residual nuclei arising from the nuclear reactions were calculated with statistical model by using Talys 1.0 and Cascade codes. Some of them are confirmed satisfactory by the half life calculations. Contaminant atoms (probably Si, Ca and Mg) in the artificial heart valve due to the fabrication process are also observed. Further experimental works in this field are highly required in order to complete a database with nuclear data required by radiotherapy [17].

REFERENCES

1. G. Kraft, Heavy ion therapy in GSI, in: U. Linz, (Editor), *Ion beams in tumor therapy*, Chapman & Hall, London, 1995, pp. 341–349.
2. J.Soltani-Nabipour *et al., Monte Carlo investigation of light-ions fragmentation in water targets,* U.P.B. Sci. Bull., Series A, **72**,*1* (2010).
3. J. Soltani-Nabipour, Gh. Cata-Danil, *Monte Carlo computation of the energy deposited by heavy charged particles in soft and hard tissues,* U.P.B. Sci. Bull., Series A, **70**, *3* (2008).
4. J. Soltani-Nabipour, D. Sardari, Gh. Cata-Danil, *Sensitivity of the Bragg Peak Curve to the Average Ionization Potential of the Stopping Medium,* Rom. Journ. Phys., **54**, *3–4*, 321–330 (2009).
5. P. Marmier, E Sheldon, *Physics of Nuclei and Particles*, Academic Press, 1969.
6. P.E. Hodgson, *Nuclear Reactions and Nuclear Structure*, Clarendon Press, Oxford, 1971.
7. A. J. Koning, S. Hilaire, M. Duijvestijn, "Talys1.0", *Proceedings of the International Conference on Nuclear Data for Science and Technology-ND 2007,* May 22–27, 2007, Nice, France.
8. F. Pulhofer, Nuclear Physics A, **280**, 267 (1977).
9. R. A. Roth, R. Katz, *Heavy Ion Beam Model for Radiobiology,* Radiation Research, **83**, 499(1980).
10. I. Kovar *et al.*, *Dosimetry of Medical Proton Beams at the JINR Phasotron in Dubna*, Communication of the Joint Institute for Nuclear research, Dubna, 1993.
11. J.F. Ziegler, J.P. Biersack, U. Littmark, *The Stopping and Range of Ions in Solids*, Vol. 1 of series *Stopping and Ranges of Ions in Matter*, Pergamon Press, New York, 1984; http://www.SRIM.org
12. IKP, Koln and DFN, IFIN-HH, Bucharest Packge.
13. A.J. Koning, M.C. Duijvestijn, Nuclear Physics A, **713**, 231 (2003).
14. A.J. Koning, S. Hilaire, S. Goriely, *Global and local level density models*, Nuclear Physics A, **810**, 13–76 (2008).
15. *** National Nuclear Data Center, Brookhaven, http://nndc.bnl.gov
16. W. Hauser, H. Feshbach, Phys. Rev., **87**, 366 (1952).
17. S.M. Qaim, *Nuclear data for medical applications: an overview*, Radiochim. Acta, **89**, 189–196 (2001).